Acta Biomaterialia 55 (2017) 455–465

Contents lists available at ScienceDirect

Acta Biomaterialia

journal homepage: www.elsevier.com/locate/actabiomat

Full length article

# Effect of e-beam sterilization on the in vivo performance of conventional UHMWPE tibial plates for total knee arthroplasty

Shine Tone [a], Masahiro Hasegawa [a,*], Giuseppe Pezzotti [b], Leonardo Puppulin [c], Akihiro Sudo [a]

[a] Department of Orthopaedic Surgery, Mie University, Graduate School of Medicine, 2-174 Edobashi, Tsu, Mie 514-8507, Japan
[b] Ceramic Physics Laboratory, Kyoto Institute of Technology, Sakyo-ku, Matsugasaki, 606-8585 Kyoto, Japan
[c] Department of Molecular Cell Physiology, Kyoto Prefectural University of Medicine, Kamigyo-ku Hirokoji Agaru, Kawaramachi-dori, 602-8566 Kyoto, Japan

ARTICLE INFO

*Article history:*
Received 28 November 2016
Received in revised form 7 March 2017
Accepted 25 March 2017
Available online 27 March 2017

*Keywords:*
E-beam sterilization
Total knee arthroplasty
UHMWPE
Oxidation
Raman spectroscopy
FT-IR
Surface damage

ABSTRACT

Although the introduction of highly cross-linked polyethylene is effective in reducing the amount of wear, there are still major concerns regarding the use of this material in total knee arthroplasty (TKA), essentially due to the reduction of fatigue resistance and toughness. Monitoring the in vivo performance of different types of UHMWPE is a much needed task to tackle the lack of information on which should be the most reliable choice for TKA. The present study was aimed at investigating the mid-term degradation of electron beam sterilized conventional UHMWPE tibial plates. Visual inspection enabled to grade the surface damage of 12 retrievals according to the Hood's score: the total wear damage correlates to the in vivo time (Spearman's $\rho = 0.681$, $p < 0.05$) and *BMI* ($\rho = 0.834$, $p < 0.001$). Surface degradation was less severe than that quantified in similar studies on $\gamma$-sterilized UHMWPE. Raman and infra-red spectroscopies were utilized to unfold the microstructural modifications. In the load zone, polyethylene whitened damage regions were noticed in the inserts implanted longer than 1 year, in which oxidation index (*OI*) is clearly higher than 1 (max 8). The maximum *OI* ($\rho = 0.802$, $p < 0.005$) and $\alpha_c$ ($\rho = 0.816$, $p < 0.005$) correlate to the implantation time in the load zone. The crystallinity increased along with the extent of oxidation. Concentration of absorbed species from synovial fluid is higher in the contact zone and correlates to maximum *OI* (Spearman's $\rho = 0.699$, $p = 0.011$). Absorption was promoted in the contact area by the mechanical action of the femoral counterpart and it exacerbated the oxidative degradation in retrievals with high concentration of absorbed species. In the non-load zone, mild but detectable oxidation was observed, probably due to free radicals trapped after sterilization.

**Statement of Significance**

Although several clinical studies on retrieved tibial bearings have been published so far, monitoring and comparing the in vivo performance of different types of UHMWPE is still a much needed task. The present study reports for the first time results on the effect of sterilization by electron beam on the mid-term in vivo performance of conventional UHMWPE tibial plates. In the present investigation, visual inspection of wear damage based on the Hood's scoring method, Raman micro-spectroscopy and Fourier-transformed infrared spectroscopy were utilized to unveil the damage, the microstructural modifications and the oxidation occurred during implantation. The findings of this investigation have been discussed and compared to previous clinical studies on $\gamma$-air sterilized, $\gamma$-inert sterilized tibial bearings.


## 1. Introduction

In the modern arthroplasty era, given the variety of orthopedic implants available on the market, surgeons are constantly facing the dilemma of which product may represent the best choice for their patients requiring joint replacement. Nevertheless, especially in the past two decades, the development of fabrication processing and the introduction of new materials aimed at ameliorating the mechanical and chemical resistance of the prosthetic components brought undisputable and tangible benefits to the patients. In this context, the advancement in design and production of UHMWPE bearings is highly representative of both the positive effort made by the orthopedic companies and the difficulty for surgeons to

* Corresponding author.
*E-mail address:* masahase@clin.medic.mie-u.ac.jp (M. Hasegawa).

http://dx.doi.org/10.1016/j.actbio.2017.03.040
1742-7061/

select the best product that fits to their needs. UHMWPE still represents the golden standard and the most reliable material to produce tibial inserts for total knee arthroplasty (TKA) [1,2], primarily because of the most favorable combination of low friction coefficient, high mechanical strength, toughness and fatigue resistance among the other biomaterials available at present [3].

The results of recent clinical studies showed that the incidence of polyethylene wear on the failure of primary TKA is clearly decreasing within the first 15 years of implantation. Sharkey et al. [4] reported a systematic retrospective review of 781 cases of revision performed between 2003 and 2012. The major causes of implant failure were identified as aseptic loosening and infection, the former predominant in the middle- and long-term retrievals, while the latter was recurrent in premature revisions (i.e., within 2 years from the primary surgery). Nonetheless, the most striking evidence was the low incidence of UHMWPE wear, which markedly decreased as compared to results obtained by the same research group in a clinical study dated back to 2002 [5]. Similar conclusions were reported by Lombardi Jr. et al. in a separate clinical study on 844 knee implants, which were retrieved during 2010 and 2011 [6]. Although the main reasons of failure by aseptic loosening in TKA were associated to poor implant design, fixation methodology and malalignment [4,6], some cases have been correlated to osteolysis triggered by the interaction of periprosthetic tissues with sub-micrometric wear debris [7–9]. Nowadays, the most established method to improve the wear resistance of UHMWPE is based on the use of ionizing radiations to generate cross-links in the microstructure of the polymer. Starting from the 1970s, when the first pioneering high-dose gamma-irradiated polyethylene liners were implanted at the Osaka Minami National Hospital in patients necessitating of total hip replacement [10], numerous studies have been conducted in order to fully understand and elucidate benefits and drawbacks of cross-linking in polyethylene for orthopedic applications [11–19]. According to the outcomes of these investigations, there is a general agreement regarding the reduction of wear in highly cross-linked polyethylene (HXLPE) liners used for total hip arthroplasty (THA) [13–16], whereas, in the case of TKA, the effects of cross-linking on the overall in vivo performance of tibial inserts is still under debate [17–21]. In fact, although HXLPE was clearly proven to be more resistant to adhesive and abrasive wear, the generation of the cross-linked polymeric network in the amorphous phase has a negative impact on fatigue resistance and toughness. The decrease of these two mechanical properties is particularly deleterious for tibial bearings, in which the cyclic contact stresses and shear forces are higher than in the case of hip liners, due to the lower conformity of the knee joint as compared to the hip [17,21]. As a result, the use of HXLPE in TKA may increase the risk of unexpected surface damages during in vivo service, such as deformation and crack propagation leading to pitting and delamination [17,22,23]. A further limiting factor that must be taken into consideration in this debate is certainly the propensity of irradiated polyethylene to long-term in vivo oxidation. In the absence of a proper post-irradiation thermal treatment, even the presence of few free radicals in the microstructure can potentially trigger the self-sustained mechanism of oxidation that degenerates over the years [24]. In addition, recent clinical studies hypothesized that the lipids absorbed during in vivo service may favor the formation of free-radicals by reacting with oxygen and, subsequently, extracting hydrogen atoms from the surrounding polyethylene chains [25–28]. It is well known that the formation of oxidized species increases the brittleness of polyethylene [29–31], which is even more threatening for HXLPE, whose mechanical resistance has already been undermined by cross-linking. For these reasons, nowadays tibial inserts made of uncross-linked UHMWPE and sterilized by non-radiative methods are still considered by surgeons as a viable choice in TKA [32–34]. In the context of the lack of a substantial number of clinical studies that may give an irrefutable answer to which kind of UHMWPE is the most advantageous in TKA, the present study was aimed at investigating the effect of sterilization by electron beam (e-beam) on the in vivo performance of uncross-linked UHMWPE tibial plates implanted for periods ranging from 3 weeks up to 8 years and 2 months. Raman (RS) and Fourier-transformed infrared (FT-IR) spectroscopies were utilized to thoroughly unveil the microstructural modifications and the oxidation occurred during exposure to the peculiar biomechanical environment of the knee. E-beam sterilization was proposed as an alternative to the more commonly used procedure based on gamma-ray. According to Blömer and Lohrmann [35], as compared to gamma-ray, e-beam sterilization has the potential to contain the generation of free radicals, namely to reduce the risk of oxidation, because the radiation process is completed in short time (i.e., few minutes) [36]. As compared to gamma sterilization, it was reported that the wear resistance of e-beam sterilized polyethylene improved after in vitro simulation testing and also the sub-surface oxidation after accelerated aging was found to be lower [35]. The present investigation was conceived to verify the in vivo performance of e-beam sterilized uncross-linked UHMWPE.

## 2. Materials and methods

### 2.1. Investigated materials

We performed experiments on a set of 12 short and middle-term retrieved tibial inserts, which were made of e-beam sterilized conventional UHMWPE that was clinically introduced in Japan since 2005 for TKA. The tibial components were machined from compression molded sheets made of GUR 1020 resin and they were terminally sterilized in $N_2$-barrier packaging by e-beam with a total dose ranging from 25 to 40 kGy, which is not sufficient to generate a highly cross-linked polymeric structure. Five retrievals were implanted within a period of one year (between 3 weeks and 8.5 months), while seven tibial inserts were embedded in vivo for more than one year (between 1.33 years and 8.17 years). Table 1 shows the list of the retrievals, including the clinical data of the patients and the cause of revision. In addition, the list includes data regarding the in vivo time and the shelf aging time in air elapsed from the revision surgery to the spectroscopic analysis (i.e., ex vivo time). Hereafter the retrieved samples will be referred using their designated number reported in Table 1. In order to investigate the modifications induced by in vivo exposure, three pristine tibial inserts were analyzed as received by the manufacturer.

### 2.2. Grading of surface damage

The twelve retrievals were examined using an optical microscope to judge the surface degradation according to the method proposed by Hood et al. [37]. The visual inspection of the bearing was also performed using a 10× and 100× magnification lens mounted on a laser/optical microscope (Keyence, VK-x200 series, Osaka, Japan), which enabled to collect micrographs using a software-assisted motorized *xy* stage. The use of laser microscope imaging enabled us to clearly visualize the surface topography of each bearing and it facilitated the discrimination and quantification of the different damage modes, which in the past relied merely on the experience of the operator. The bearing surface was divided in 10 sections as described by Hood et al. [37]. During the visual inspection of each section, the following seven modes of surface degradation were considered for grading: embedded debris, scratching, delamination, surface deformation, abrasion, burnish-

**Table 1**
List of the retrievals, including the clinical data of the patients.

| Sample | Gender | Age | Ope side | In vivo time (mo/yr) | Ex vivo time (mo/yr) | Diagnosis | Weight (kg) | BMI (kg/m$^2$) | Varus or Valgus | Insert type/ Thickness (mm) | Cause of revision |
|---|---|---|---|---|---|---|---|---|---|---|---|
| 1 | Female | 75 | Right | 0.7/0.06 | 42.0/3.50 | OA | 53 | 23.9 | 1°valgus | UC/10 | Patella fracture |
| 2 | Female | 75 | Left | 0.7/0.06 | 33.6/2.80 | OA | 53 | 23.9 | 3°valgus | PS/12 | Patella tendon rupture |
| 3 | Male | 68 | Left | 5.0/0.42 | 27.6/2.30 | RA | 52 | 20.8 | 2°varus | UC/18 | Infection |
| 4 | Male | 68 | Left | 7.0/0.58 | 31.2/2.60 | RA | 52 | 20.8 | 2°varus | UC/10 | Infection |
| 5 | Male | 51 | Right | 8.5/0.71 | 24.0/2.00 | OA | 83 | 30.3 | 1°varus | UC/10 | Infection |
| 6 | Male | 83 | Right | 16.0/1.33 | 32.0/2.67 | OA | 56 | 22.2 | 0° | PS/12 | Infection |
| 7 | Male | 72 | Left | 28.0/2.33 | 12.0/1.00 | RA | 52 | 20.8 | 2°varus | UC/18 | Infection |
| 8 | Female | 66 | Left | 30.0/2.50 | 29.0/2.42 | OA | 76 | 33.8 | 3°varus | PS/14 | Infection |
| 9 | Female | 84 | Right | 61.0/5.10 | 3.9/0.33 | OA | 60 | 26.3 | 2°valgus | PS/16 | Hemarthrosis |
| 10 | Female | 78 | Left | 74.0/6.20 | 3.5/0.29 | OA | 55 | 26.9 | 1°valgus | PS/14 | Infection |
| 11 | Female | 93 | Right | 75.0/6.25 | 2.7/0.23 | OA | 64 | 28.4 | 1°valgus | PS/12 | Infection |
| 12 | Female | 84 | Right | 97.4/8.17 | 1.5/0.13 | OA | 47 | 25.4 | 1°valus | PS/18 | Infection |

OA (osteoarthritis), RA (rheumatoid arthritis), PS (posterior stabilized), and UC (ultra-congruent).

ing and pitting. For each mode and each section, the severity of the damage was graded according to the percentage of area covered by damages. The scale of this grading system was established from 0 to 3, where the grade of 0 means absence of damages on the surface, while grades of 1, 2 and 3 correspond to 10, 10–50, and over 50% of the section area covered by damages, respectively. In other words, for a single damage mode, if it was graded 3 in each of the 10 sections, its total damage score in that particular tibial insert would be $3 \times 10 = 30$. Considering 7 different damage modes, the highest total damage score (TDS) for one tibial plate would be $30 \times 7 = 210$.

### *2.3. Raman spectroscopy*

In-plane hyperspectral Raman maps were collected from the surface and sub-surface of the tibial inserts to visualize the microstructure of the polymer in terms of phase fractions. The analyses were performed using a microprobe spectrometer (T-64000, Horiba/Jobin-Yvon, Kyoto, Japan) in back-scattering geometry, which enabled to collect spectra at different depths within the surface of the samples in a nondestructive way. The excitation source was a 532 nm diode laser (SOC Juno, Showa Optronics Co., Ltd, Tokyo, Japan) yielding a power of approximately 9 mW on the UHMWPE surface. The confocal configuration of the probe adopted throughout the present experiments corresponded to a $100 \times$ objective lens; the pinhole diameter of the cross slit was fixed as 100 μm. The recorded non-polarized spectra were averaged over three successive measurements at each selected location. A spectral resolution better than 0.15 cm$^{-1}$ was achieved by means of an 1800 lines/mm grating. The volume fractions of crystalline ($\alpha_c$), amorphous ($\alpha_a$) and third phase fractions ($\alpha_t$), were calculated using the method introduced by Strobl and Hagedorn [38], which is based on a set of equations that includes the unpolarized intensities of vibrational bands located at 1296, 1305, and 1414 cm$^{-1}$, as follows [38–40]:

$$\alpha_c = \frac{I_{1414}}{0.46 \times (I_{1293} + I_{1305})} \tag{1}$$

$$\alpha_a = \frac{I_{1305}}{(I_{1293} + I_{1305})} \tag{2}$$

$$\alpha_t = 1 - (\alpha_c + \alpha_a) \tag{3}$$

The third phase in polyethylene can be summarily described as an anisotropic phase located at the interface between amorphous and crystalline phases, in which the molecular chains are aligned along the same direction but they lost their lateral order [38]. At first, the retrievals were investigated in a nondestructive way by collecting maps of Raman spectra on the surface of two different locations: the medial wear zone and the non-load zone (i.e. region between medial and lateral contact areas). Fig. 1 (a) shows the schematic explaining the experimental routine followed to collect the Raman spectra. At each selected depth, a map $50 \times 50$ μm$^2$ in dimension was collected with an in-plane sampling of 5 μm step (for a total of $11 \times 11 = 121$ non-polarized spectra per each map). Following the nondestructive characterization, the tibial inserts were sectioned through their thickness to obtain microtomed sections from the medial wear zone and non-wear zone. Each slice

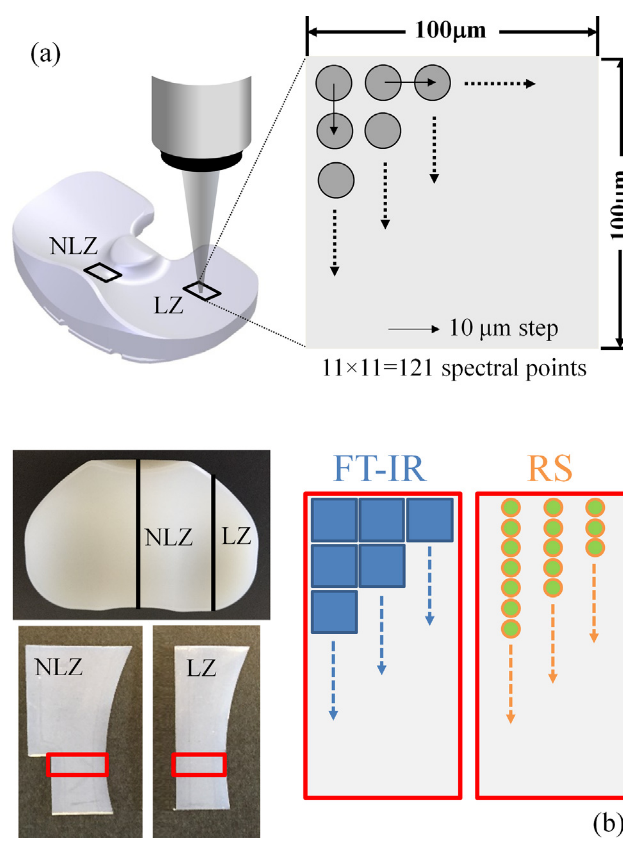


**Fig. 1.** (a) Schematic explaining the experimental routine followed to collect the Raman spectra from the surface of the load (L) and non load (NL) zones. A total of n = 121 measurements were collected by the three pristine samples. (b) Microtoming procedures for the preparation of the slices and the experimental routine used for their spectroscopic analyses.

was 200 μm thick. The Raman microscopic analysis of these samples enabled to calculate detailed profiles of crystalline, amorphous and third phase fractions along the thickness of the tibial component. For each slice, three line scans of Raman spectra were collected from the sliding upper surface to the bottom surface of the bearing component, with sampling of 100 μm step. A brief description of the cutting procedures for the preparation of the microtomed slices and the experimental routine used for their spectroscopic analyses is given in Fig. 1 (b).

### 2.4. FT-IR spectroscopy

The microtomed sections were preliminarily characterized by Fourier Transform Infrared Spectroscopy (FT-IR) following experimental protocols similar to those used for the Raman analysis (see Fig. 1 (b)). FT-IR analysis was carried out using the imaging system Spotlight 200 (Perkin Elmer, Waltham, Massachusetts, USA). FT-IR spectra of polyethylene were acquired at aperture size of 200 × 200 μm$^2$. The oxidation of the polymer was estimated according to the standard ASTM 2102 [41], which defined an oxidation index (*OI*) as the ratio of the area under the carbonyl peak at around 1720 cm$^{-1}$ to the area under the $CH_2$ absorption peak centered around 1370 cm$^{-1}$. The assessments were made before and after extraction of contaminants from the retrievals by soaking the slices in boiling hexane (69 °C) for 18 h. The purpose of the FT-IR analyses was twofold: (i) to create *OI* profiles as a function of depth away from the sliding surface of the tibial insert, which enabled us to judge the oxidative degradation of beta-sterilized UHMWPE; (ii) to obtain the phenomenological correlation between *OI* and crystallinity fraction ($\alpha_c$), based on protocols validated in a recently published paper [42]. The adopted experimental routine was conceived as follows: three line scans were collected from the sliding surface to the back-surface of the tibial inserts with 200 μm steps. For each slice and at each depth, the *OI* was calculated as the average of 3 measurements. A further assessment was obtained by subtracting the value of *OI* calculated before treatment by hexane to that calculated after treatment, which is a parameter correlated to the concentration of absorbed species from the synovial fluid. The maximum value of this parameter was obtained for each sample (hereafter referred as Extracted Species Index, $ESI_{\max}$), both in the load and non-load zones.

### 2.5. Statistical analysis

Non-parametric Spearman analysis was used to estimate the statistical correlation between TDS and body mass index (*BMI*); TDS and implantation-time; maximum oxidation index ($OI_{max}$) and implantation time; maximum crystallinity ($\alpha_{c,max}$) and implantation time; $OI_{max}$ and $ESI_{\max}$; $\alpha_{c,max}$ and $ESI_{\max}$. The polyethylene phase fractions calculated from the surface by Raman Spectroscopy are presented as the mean of n = 121 independent measurements ± standard deviation (SD). Differences between pristine and retrievals were statistically validated using non-paired *t*-test (p = 0.05). All statistical analyses were performed with EZR (Saitama Medical Center, Jichi Medical University, Saitama, Japan), which is a graphical user interface for R (The R Foundation for Statistical Computing, Vienna, Austria).

## 3. Results

The visual inspection of the bearing surfaces enabled to grade the severity of the wear degradation according to the Hood's TDS, which is reported in Fig. 2 for each sample. Only sample 3 was graded as 0, which means absence of damage on the surface, while samples 1, 2 and 4, which were also short-term retrievals,

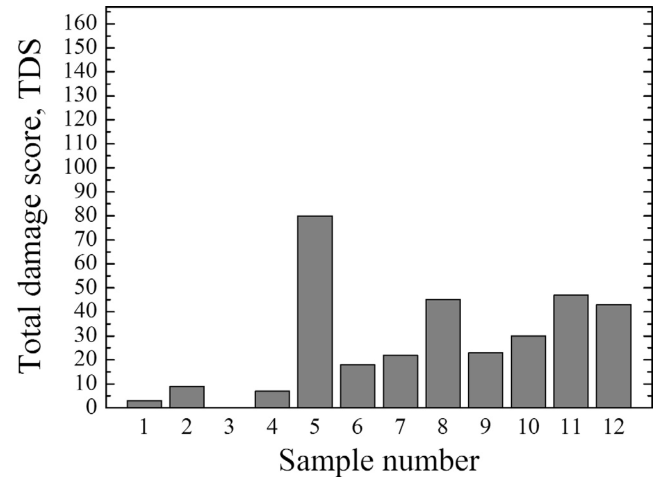


**Fig. 2.** Hood's total damage score (TDS) as calculated from each retrieved tibial insert.

revealed very low degradation of the surface. The mid-term retrievals clearly showed increasing damage scores. The only outlier was sample 5, which was characterized by the most widespread presence of surface damages, although it was implanted for less than one year. Fig. 3 reports examples of different typologies of wear damage observed on the surface of the retrievals. This analysis showed the presence of all the seven modes of surface degradation, namely: embedded debris, scratching, delamination, surface deformation, abrasion, burnishing and pitting.

Fig. 4 (a) and (b) show the TDS as a function of the patients' *BMI* and implantation time, respectively. The non-parametric Spearman's test confirmed the monotonic relationship in both cases. The correlation was particularly strong between the extent of wear and *BMI* (Spearman's $\rho = 0.834$, $p < 0.001$). In Table 2 we reported the mean damage scores calculated for each singular damage mode, which were also compared to those presented by Kelly et. al. [43] for mobile tibial bearing made of γ-barrier sterilized conventional UHMWPE (Sigma, DePuy, Warsaw, IN). The non-destructive analysis by Raman spectroscopy was designed to visualize the evolution of the polyethylene microstructure after implantation on the surface and subsurface of the retrievals. In Fig. 5 (a)-(c) and (d)-(f), the mean fractions of crystallinity, amorphous phase and third phase are shown as calculated from the load zone and non-load zone of the 12 retrievals, respectively. In each plot of Fig. 5, the red lines correspond to the mean phase fractions obtained from the three pristine tibial inserts. On the surface of the worn area, the most of the retrievals showed the clear increase of crystallinity and amorphous phase at the expense of the third phase (i.e., Samples 1, 2, 3, 4, 6, 9, 10, 12). Sample 8 revealed the highest increase of crystallinity, which induced the reduction of both the amorphous and third phase. Conversely, only samples 5, 11 and 7 were characterized by reduction of the orthorhombic crystalline phase. Also on the surface of the non-contact area, the crystallinity increased in the most of the samples, mainly accompanied by the reduction of the third phase. Only sample 8 showed a slightly different structural modification, in which also the amorphous phase was greatly lower than the value calculated from the pristine. At the completion of the non destructive characterization of the bearings, the samples were cut and microtomed to carry out comparative analysis by Raman and FT-IR spectroscopies. In Fig. 6 (a) and (b) are reported examples of phase fractions and *OI* profiles that these two spectroscopic techniques enabled to calculate from two slices obtained from one of the pristine samples and the load zone of Sample 8, respectively. We also reported the optical images

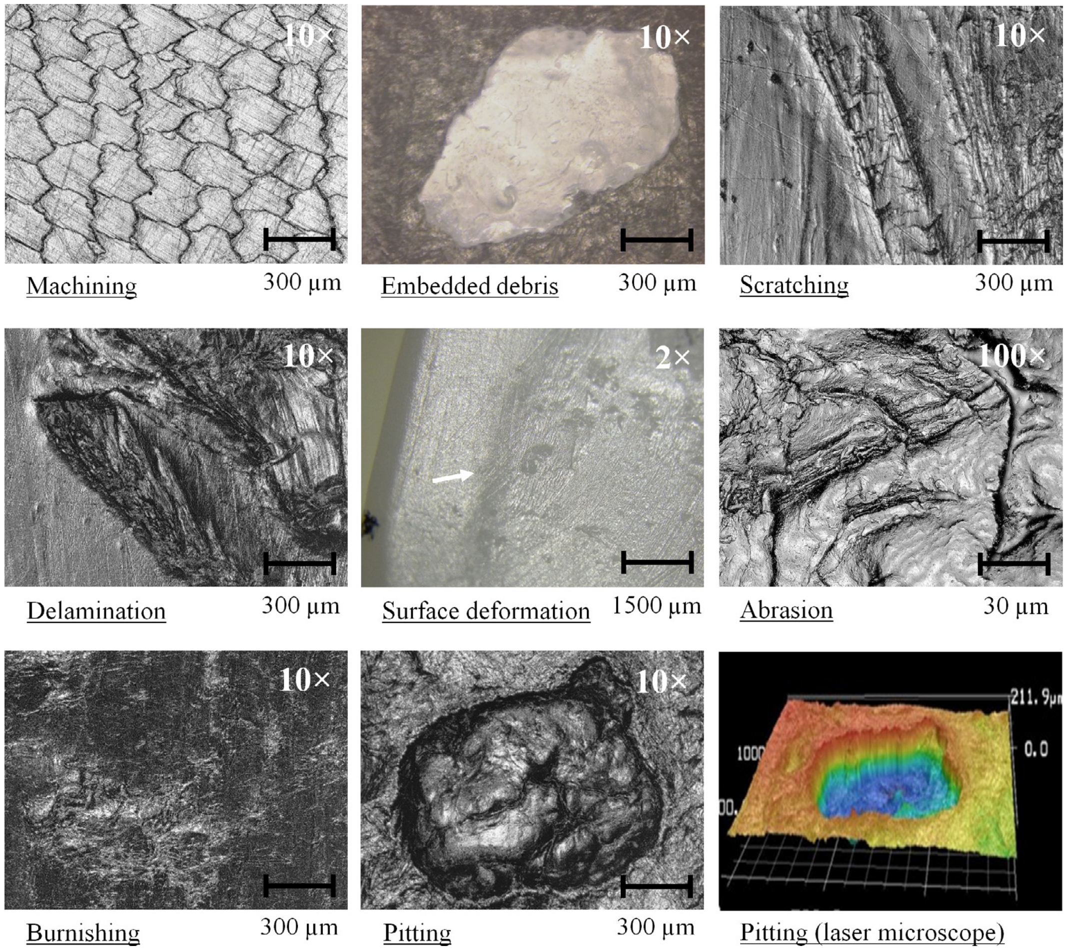


**Fig. 3.** Different typologies of wear damage observed on the surface of the retrievals. For the surface deformation, the feature of the damage is pointed by the white arrow.

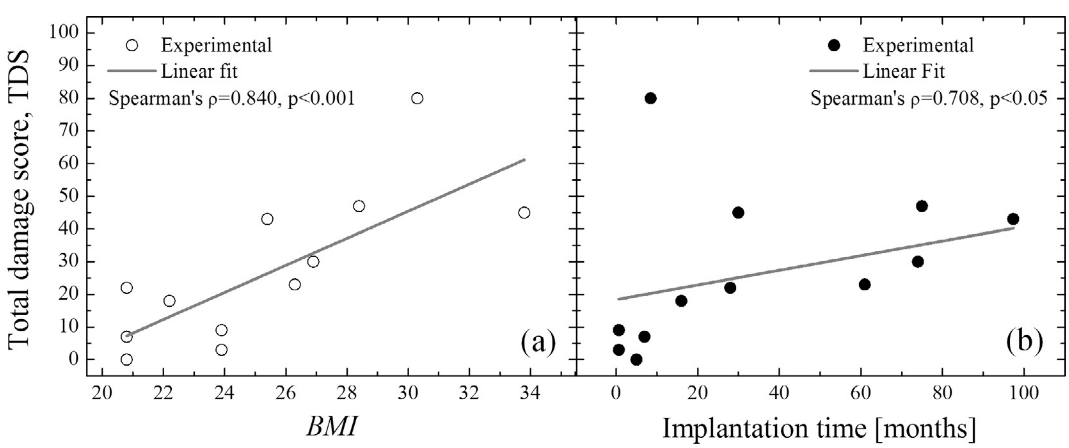


**Fig. 4.** Plots of total damage score (TDS) as a function of patients' *BMI* (a) and implantation time (b).

of the slices, which indisputably show the presence of "white bands" near the sliding surface and the back-surface of the retrieval. The thickness of each band clearly matches the range of depths in which the spectroscopic assessments indicated the major microstructural variations and oxidative degradation. Based on a protocol that we validated and explained in detail in a recently published study [42], the correlation between oxidation and variation of orthorhombic phase was obtained for this specific type of UHMWPE by considering the entire set of data collected from the slices of every samples (see Fig. 7). In order to elucidate the correlation between the chemical/physical degradation of the polymer and the time of exposure to the biological environment, we considered $OI_{max}$ and $\alpha_{c,\max}$ calculated from each retrieved sample during the analysis of the slices. Fig. 8 (a) and (b) shows plots of $OI_{max}$ and $\alpha_{c,max}$ as a function of in vivo implantation time, respectively. Data were discriminated depending on the presence of load during in vivo service. The correlation between variables was verified by calculating the Spearman's ρ coefficients, which are also reported

**Table 2**
Mean damage scores by damage mode calculated for e-beam- and γ-barrier sterilized tibial plates.

| Damage mode | E-beam-barrier sterilized Mean damage score (n = 12) | γ-barrier sterilized (Ref. [43]) Mean damage score (n = 48) |
|---|---|---|
| Pitting | 5.2 ± 3.3 | 9.9 ± 6.1 |
| Embedded debris | 0.1 ± 0.3 | 0.6 ± 1.1 |
| Scratching | 6.7 ± 3.3 | 8.9 ± 4.6 |
| Delamination | 0.2 ± 0.6 | 0.0 ± 0.0 |
| Surface deformation | 2.0 ± 2.6 | 0.1 ± 0.6 |
| Burnishing | 1.9 ± 3.0 | 18.1 ± 5.2 |
| Abrasion | 1.1 ± 2.3 | 0.5 ± 1.3 |

in Fig. 8. In the load zone, both $OI_{max}$ and $\alpha_{c,max}$ strongly correlate to the implantation time, while in the non-load zone the correlation was weak, although still significant in the case of $OI_{max}$. All the data showed in Figs. 6–8 were collected from slices after extraction treatment. The FT-IR assessments performed before boiling the slices in hexane were useful to estimate the absorption of species from the synovial fluid in each retrieved tibial insert. Fig. 9 shows examples of typical FT-IR spectra collected from slices of one pristine tibial plate and the medial load zone of Sample 7 before and after extraction. Among the different species containing carbonyl groups that contribute to the total intensity of the infrared band centered at around 1720 $cm^{-1}$, species extracted from the retrievals are mainly esters, acids and unsaturated lipids, which absorb at around 1740 and 1710 $cm^{-1}$ [44]. At these vibrational frequencies, the spectra of Sample 7 in Fig. 9 clearly show reduction of C=O stretching intensity after boiling in hexane for 18 h. For each retrieval, Fig. 10 (a) and (b) report the $OI_{max}$ calculated after lipid extraction as a function of the respective $ESI_{max}$ in the load and non-load zones, respectively. In these figures, different symbols were used to highlight data obtained from retrievals with different implantation time. Samples 8 and 12 were also explicitly indicated

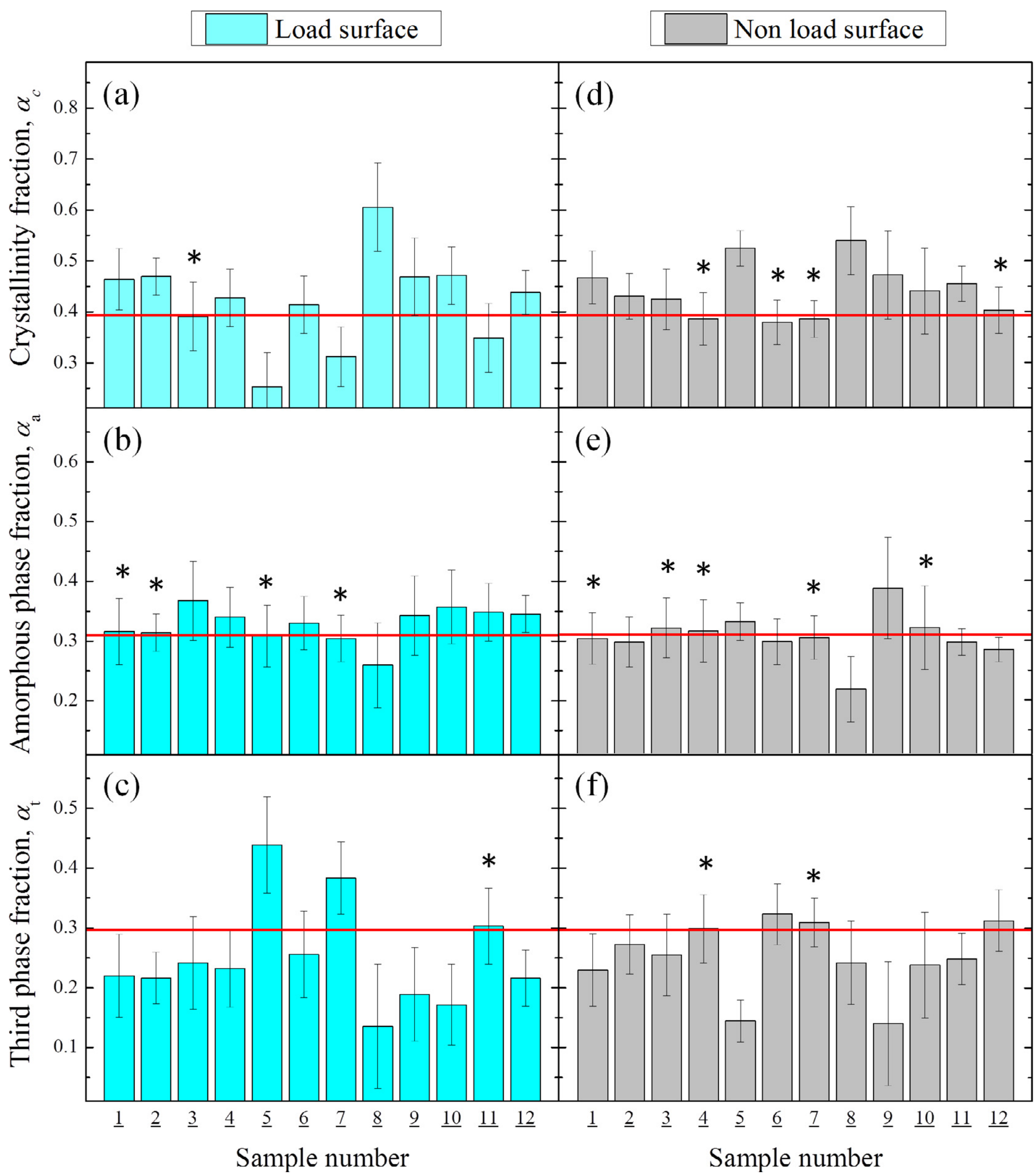


**Fig. 5.** Crystallinity (a), amorphous phase (b) and third phase (c) fractions as calculated from the load zone of the 12 retrievals. Similarly, in (d)–(f) are shown the fractions from the non load zones. For each sample and surface, the mean fraction has been compared to the mean calculated from the three pristine samples using Student's *t*-test (n = 121, 95% confidence level). No statistically difference between the means (p > 0.05) have been marked by *.

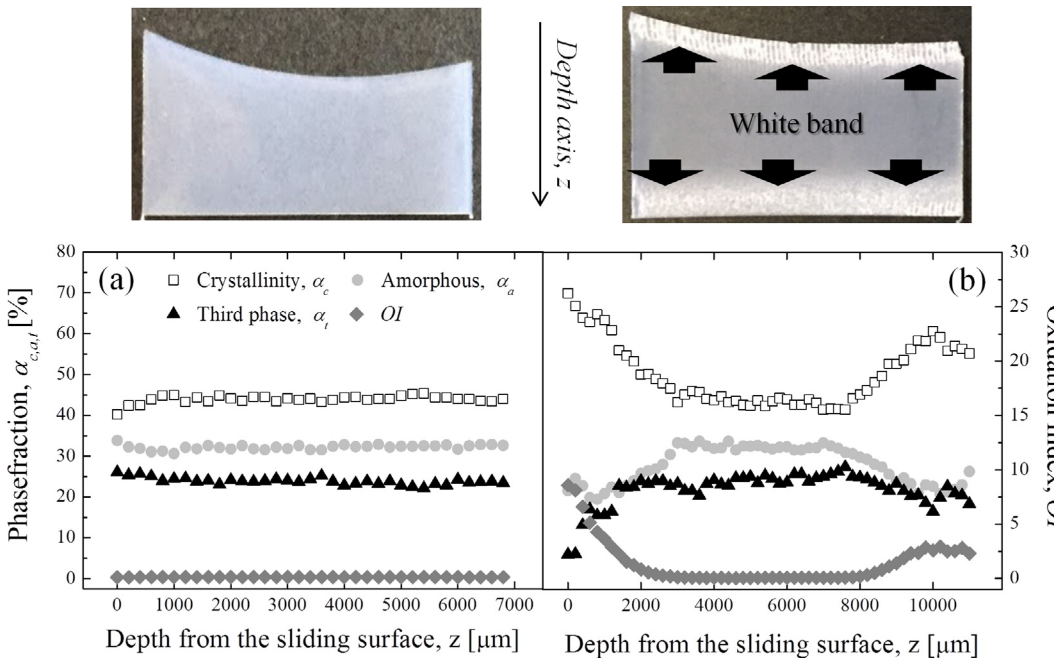


**Fig. 6.** Examples of phase fractions and *OI* profiles retrieved from two slices of one pristine sample (a) and the load zone of sample 8 (b).

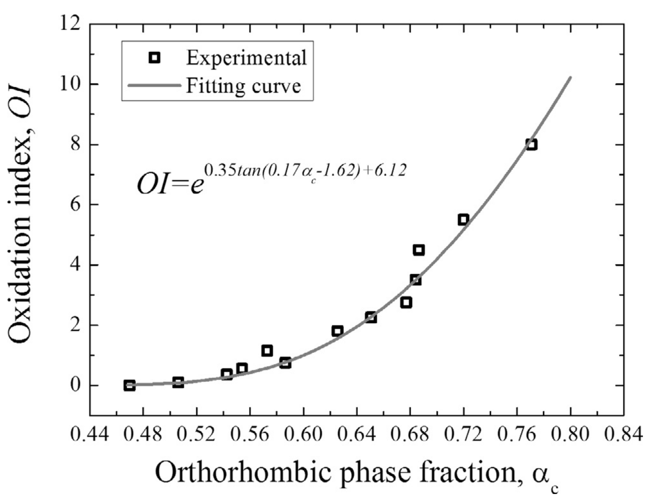


**Fig. 7.** Phenomenological correlation between *OI* and crystallinity fraction ($\alpha_c$) for e-beam conventional UHMWPE, based on protocols recently validated [42].

in the figure, since they showed the highest $OI_{max}$ and $ESI_{max}$ both in the load and non-load zone. The range of variation of $ESI_{max}$ in the contact zone (i.e., from 0.16 to 1.91) was much wider than that measured from the non-contact zone (i.e., from 0 to 0.47). Overall, concentration of the extracted species correlates to the exacerbation of the in vivo oxidative degradation only in the part of the bearing that carried the mechanical load (Spearman's $\rho = 0.699$, $p = 0.011$).

## 4. Discussion

### *4.1. Surface damage*

The purpose of this study was to investigate the in vivo performance of e-beam sterilized conventional UHMWPE tibial inserts with follow-ups ranging from few months to 8 years. The most recurrent cause of revision was infection and none of the patients suffered of complication related to extensive wear of the implant. The visual investigation of the bearing surfaces was aimed at evaluating the damage patterns and clarifies the most recurrent modes

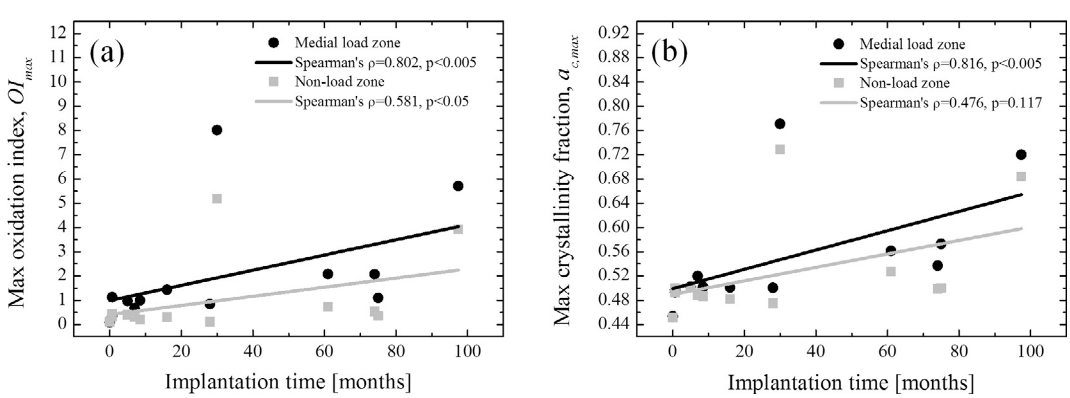


**Fig. 8.** $OI_{max}$ (a) and $\alpha_{c,max}$ (b) as a function of in vivo time in the load and non load zones.

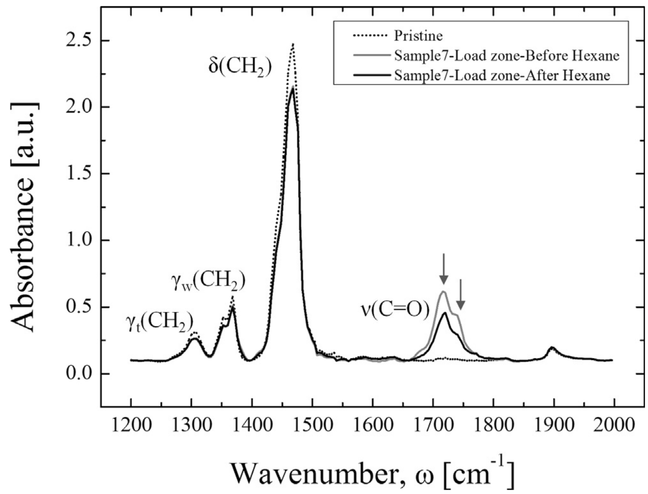


**Fig. 9.** Examples of FT-IR spectra collected from the pristine and the load zone of Sample 7 before and after boiling in hexane for 18 h. The two arrows highlight the reduction of intensity in the C=O stretching region due to lipid extraction ($\gamma_w$ = wagging; $\gamma_t$ = twisting; δ = bending; ν = stretching [67]).

of surface degradation triggered by wear. The experimental evidences reported in Figs. 2–4 suggest the onset of wear degradation within few months of implantation, although its extent was very small. The wear damage became clearly more widespread in the mid-term tibial inserts, but it did not much vary among these samples (see Fig. 2). Similar trends were reported in a previous study on retrieved tibial inserts made of UHMWPE sterilized by different methods (i.e., gas plasma and γ-ray), in which the roughness of the bearing surface increased after the first year of implantation, but did not vary significantly for longer follow-ups [45]. The only outlier was sample 5, which had been implanted for 8.5 months and showed the highest TDS (i.e., almost as twice as much the highest score evaluated among the mid-term retrievals). Such a deviation from the results of the other samples might be explained considering that the patient was the heaviest, 83 kg, and the youngest, 51 years, namely an age in which, normally, patients are still active. Previous studies on retrieved tibial inserts made of conventional UHMWPE sterilized by γ-ray in inert atmosphere showed average TDS of 59 ± 22 for n = 71 retrievals with follow-up less than 1 year [46] and 38 ± 10 for n = 48 mid-term retrievals with mean in vivo time of 3 ± 2 years [43]. In the present study, we obtained the average TDS of 26 ± 22 for n = 12 e-beam sterilized tibial inserts with mean follow-up of 2.8 ± 2.8 years, namely comparable to the implantation time reported in Ref. [43]. Overall, the correlation between TDS and the implantation time was statistically meaningful, but very moderate, as can be inferred by the low slope of the fitting line. In addition, meaningful correlation was obtained considering the *BMI*, which suggests that the patient variable may affect the in vivo performance of knee replacements. Conversely, in the study of mid-term γ-barrier sterilized polyethylene retrievals [43], TDS did not statistically correlate to BMI and implantation time. As shown in Table 2, scratching and pitting were the two most frequent types of damage, which is the experimental evidence also observed in γ-sterilized conventional UHMWPE [43,46]. Since the sample size in our study is smaller than those reported in Refs. [46] and [43], the conclusions based on these results require further confirmation to be considered definitive.

### 4.2. Spectroscopic microstructural analysis

As a general point of view, UHMWPE used in total joint arthroplasty has been proven to possess excellent mechanical properties as long as its unoxidized state is preserved [13,14,47–50]. For this reason, monitoring the microstructural modifications induced by exposure to real physiological loads and biological environment as a function of implantation time can be considered as a fundamental approach to understand and clarify the reduction of performance in knee bearing components during the long term. The results of the spectroscopic assessments showed in the present study demonstrate that the combined use of Raman and FT-IR techniques is a viable tool to elucidate the causes and the consequences of wear degradation. On the surface of the load zone, modification of the microstructure can manifest as a result of the combined effect of high plastic deformation and oxidative degradation. Oxidation can trigger recrystallization by breaking the molecular chains, lowering their molecular weight and therefore enhancing their mobility and their rearrangement in organized lamellar structures [42,51–55]. High stresses on the surface may induce loss of anisotropy in the crystalline phase and third phase. In fact, adjacent crystalline lamellae are interconnected by tie molecules, which enable load transfer and are embedded into the amorphous network. High plastic deformation occurs within the first microns of the worn surface and it increases the load transfer, whose consequences can be twofold: i) loss of anisotropy in the crystalline phase and/or third phase, namely the formation of new isotropic amorphous phase [56–59]; ii) loss of lateral order in some molecular chains of the orthorhombic crystalline structure, namely increase of the third phase. The overall increase of orthorhombic phase showed in Fig. 5 (a)-(c) indicates that oxidation-induced recrystallization occurred on the surface; while

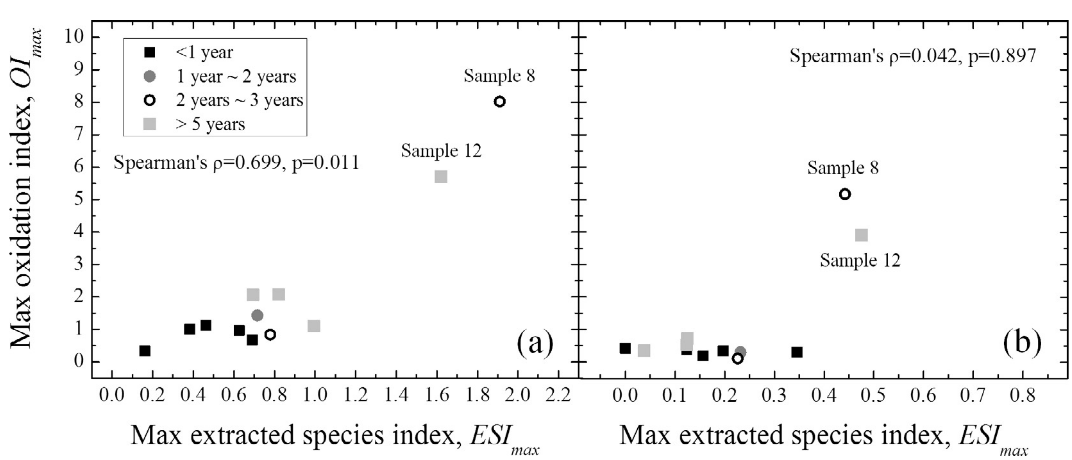


**Fig. 10.** For each retrieved sample, $OI_{max}$ calculated after lipid extraction as a function of the respective $ESI_{max}$ in the load (a) and non-load (b) zones.

the fact that the amorphous phase increased in several samples suggests that also plastic deformation simultaneously contributed by reducing the third phase and/or part of the crystalline phase. Samples 5 and 7 are two exceptions, in which the crystallinity decreased and the third phase increased, probably due to relevant plastic deformation that disrupted the lateral order in some lamellae (i.e., patient of sample 5 was the youngest and the heaviest). The general trends observed in the non-load zones (see Fig. 5 (d)-(f)) indicates that recrystallization occurred especially on the surface of the mid-term retrievals, due to the onset of oxidation. On average, the amorphous phase did not increase, while the oxidative degradation reduced the amount of the third phase. Such experimental evidence suggests that recrystallization occurred only in the third phase, leading to lamellar thickening, since it is the anisotropic phase enclosing the lamellae and separating them from the amorphous phase. One important factor to take into consideration in the evaluation of the data in Fig. 5 is the ex-vivo time of each sample. In fact, recent studies pointed out that oxidation can remarkably increase during shelf storage after implantation [25] and after accelerated aging following implantation [26] even in highly cross-linked and remelted polyethylene, which did not show trace of free radicals before implantation and also minimal oxidation at the time of explantation. As far as our samples are concerned, as shown in Table 1, the mean shelf storage time in air for the short-term retrievals was 31.7 ± 6.8 months, while for the mid-term samples it was 12.1 ± 13 months. Muratoglu et al. [25] reported that the ex-vivo oxidation occurred in remelted HXLPE retrievals within 12 months of shelf aging in air was still negligible (i.e., *OI* estimated at around 0.1), suggesting that, in the present study, only the ex-vivo time of the short term samples (i.e., time in vivo less than 2 years) may have led to overestimate the actual oxidation levels reached during implantation. As an exception, Sample 8 had an ex vivo time of 2.43 years, namely, according to Ref. [25], we may estimate an increase of $OI \approx 1$, which is still not sufficient to deny a major contribution to the total oxidation brought by different factors. Currier et al. [60] presented interesting results on 67 γ-barrier sterilized conventional UHMWPE bearings with follow-ups of 0.1 to 8.2 years, which are comparable to those presented in our study. The γ-barrier sterilized bearings were analyzed less than 6 months after retrieval and they showed average ketone index (*KI*) of 0.180 ± 0.197, corresponding to $OI_{max} = 0.344$, since $OI = 1.91 \times KI$ [61]. The 12 retrievals investigated in the present study showed an average $OI_{max} = 2.1 \pm 2.3$, which is higher than the peak of oxidation measured in Ref. [60]. Similar results on γ-barrier sterilized polyethylene were presented by Medel et al. [62], which also analyzed 29 tibial inserts made of γ-air-sterilized conventional UHMWPE (GUR415 and 1900H) with time ex-vivo less than 1 year and average time in vivo of 11.6 years. These samples showed an average $OI_{max}$ of 3.5 ± 1.9 in the medial load-zone, which is similar to the mean $OI_{max}$ measured in the mid-term retrievals of our study (i.e., 3.3 ± 2.9), although it is important to notice that our average in vivo time was barely twice as shorter (5.1 ± 2.2 vs. 11.6 years). Based on these result**s**, in the mid-term follow-up, e-beam-barrier sterilized conventional UHMWPE showed, respectively, inferior and not superior resistance to oxidative degradation than γ-barrier and γ-air sterilized conventional UHMWPE. The whitened regions observed near the sliding surface and back surface of several mid-term retrievals, as shown in Fig. 6, clearly confirmed the onset of oxidation after few years of exposure to the biological environment. The peaks of oxidation and crystallinity were detected close to the surface and they showed strong correlations with the implantation time in the load zone (see Fig. 8 (a)), proving that the mechanical action of the femoral counterpart had actively participated to the oxidative degradation of the microstructure. Overall, in the non-load zone the oxidation was low, namely less than 1, that is the critical level at which the degradation of the mechanical properties becomes an issue [63]. The in vivo generation of free-radicals and the unexpected oxidation observed in the mid-term exposure may be correlated to the lipids contained in the synovial fluid. Costa et al. [44] reported that lipids, such as squalene and cholesterol, commonly diffuse from the synovial fluid into the UHMWPE component during in vivo service. It has been already hypothesized in previous studies that the unsaturations of these species may react with oxygen and abstract hydrogen atoms from the surrounding polyethylene chains, inducing the generation of free radicals in the polymer [25–27]. The clinical relevance of this phenomenon is yet to be fully elucidated and it is still under debate. Since lipids are one of the main species extracted from retrievals [44], in the present study we assumed that increasing $ESI_{max}$ corresponds to increasing concentration of unsaturated lipids absorbed into the microstructure, although part of the extracted carbonyl groups can be attributed to esters and carboxylic acids formed after oxidation [44]. The data presented in Fig. 10 (a) and (b) show that the concentration of extracted species was higher in the load zone as compared to the non-load zone, meaning that the pressure of the femoral component on the lubricating synovial fluid enhanced lipid absorption. The average $ESI_{max}$ calculated from the load zones of the 12 samples was 0.82 ± 0.49, while it was 0.21 ± 0.15 in the case of the non-load zone. Overall, $ESI_{max}$ and $OI_{max}$ showed statistically significant correlation only in the contact zone ($\rho = 0.699$), but independently on the implantation time. In fact, the retrieval implanted for 2.5 years (i.e., Sample 8, $BMI = 33.8$) showed the highest $ESI_{max}$ and $OI_{max}$ in the load zone, suggesting that the patient variable affects the extent of species absorbed from the synovial fluid into the microstructure of the tibial component. Moreover, as previously stated, the expected ex-vivo contribution to oxidation measured in our mid-term samples can be considered as negligible. In light of these considerations, the results reported in Fig. 10 (a) and (b) suggest that in vivo oxidation may have been promoted by lipid absorption. In the non-load zone, severe oxidation was measured only in mid-term retrievals with $ESI_{max} > 0.4$ (i.e., Samples 8 and 12), which may indicate that the generation of free radicals triggered by oxygen reactive species (i.e., lipids) is relevant only if a certain concentration threshold is exceeded. Indeed, the levels of oxidation reached in these two samples are much higher than those typically observed in UHMWPE sterilized in air by radiative methods and analyzed after 10 years of shelf aging [29] or accelerated aging [64,65], namely without any presence of lipids. In addition, it is worth mentioning that the oxygen availability in the load zone is supposed to be lower than in the non-load zone, which is permanently in contact with abundant oxygen-containing body fluid [66]. Such a factor may explain the higher $OI_{max}$ measured in the non-load zones of Samples 8 and 12 as compared to the load-zones of the other mid-term retrievals at similar levels of $ESI_{max}$. Conversely, in the load-zone of Samples 8 and 12, the high concentration of absorbed species promoted by the cyclic load and the combined effect of the mechanical deformation may be the cause of the severe oxidative degradation of the polymer. Further studies are necessary to quantify the extent of lipid and cyclic load contributions to the in vivo oxidation of UHMWPE. In particular, the discrimination and quantification of each type of extracted species from retrievals take on pivotal importance in confirming the mutual correlation between unexpected in vivo oxidation and lipids.

## 5. Conclusion

Twelve retrieved tibial bearings made of e-beam sterilized conventional UHMWPE were thoroughly analyzed to evaluate the surface damage and to unfold the microstructural modifications induced by wear and oxidative degradation. None of the revision surgeries was caused by issues related to wear. The follow-ups of the retrievals ranged from few months up to 8 years, which enabled to obtain meaningful correlations between some features of the material degradation and the implantation time. The visual inspection of the bearing surface enabled to quantify the wear damage according to the Hood's damage score, which correlates to the in vivo time. The surface degradation was less severe than that quantified and presented in similar studies on $\gamma$-barrier sterilized UHMWPE. The spectroscopic analyses by Raman and FT-IR techniques visualized the effect of the in vivo exposure on the microstructure of the polymer, which clearly underwent to modifications exacerbated as a function of implantation time. The resistance to oxidative degradation was inferior to that observed in previous studies on $\gamma$-barrier sterilized tibial plates with similar mean implantation time, but comparable to that of $\gamma$-air sterilized tibial plates. The conclusions based on the comparison of e-beam sterilized UHMWPE to the other types of UHMWPE for TKA during in vivo service requires a larger sample size to be confirmed. In the load zone of the bearing, the appearance of polyethylene whitened regions was noticed close to the surface in 6 of the 7 mid-term retrievals, with follow-ups longer than 1 year. In these regions, the levels of *OI* were clearly higher than 1, reaching the maximum value of 8 in one sample. The crystallinity increased along with the extent of the oxidation. Such a microstructural modification is tangibly associated to the loss of mechanical properties (i.e., embrittlement of the polymer). Synovial fluid absorption was promoted in the contact area by the mechanical action of the femoral counterpart and, combined to mechanical stress, it exacerbated the oxidative degradation. In the non-load zone, mild but detectable oxidation was observed, probably induced by the presence of free radicals after sterilization. The presence of species absorbed from the synovial fluid was less detrimental than in the case of the load zone, possibly because of the conspicuously lower concentration and the absence of mechanical stress that can assist the reaction of unsaturated bonds and formation of free radicals.

## References


[1] M. Ritter, The Anatomical Graduated Component total knee replacement A LONG-TERM EVALUATION WITH 20-YEAR SURVIVAL ANALYSIS, J. Bone Joint Surg., Br. 91 (6) (2009) 745–749.

[2] H.-M. Ma, Y.-C. Lu, F.-Y. Ho, C.-H. Huang, Long-term results of total condylar knee arthroplasty, J. Arthroplasty 20 (5) (2005) 580–584.

[3] M. Kutz, Applied Plastics Engineering Handbook: Processing and Materials, William Andrew, 2011.

[4] P.F. Sharkey, P.M. Lichstein, C. Shen, A.T. Tokarski, J. Parvizi, Why are total knee arthroplasties failing today—has anything changed after 10 years?, J Arthroplasty 29 (9) (2014) 1774–1778.

[5] P.F. Sharkey, W.J. Hozack, R.H. Rothman, S. Shastri, S.M. Jacoby, Why are total knee arthroplasties failing today?, Clin Orthop. Relat. Res. 404 (2002) 7–13.

[6] A. Lombardi Jr., K. Berend, J. Adams, Why knee replacements fail in 2013 patient, surgeon, or implant?, Bone Joint J 96 (11 Suppl. A) (2014) 101–104.

[7] J. Gallo, S.B. Goodman, Y.T. Konttinen, M.A. Wimmer, M. Holinka, Osteolysis around total knee arthroplasty: a review of pathogenetic mechanisms, Acta Biomater. 9 (9) (2013) 8046–8058.

[8] S.M. Kurtz, The clinical performance of UHMWPE in knee replacements, in: UHMWPE Biomaterials Handbook, 2009.

[9] G.R. Scuderi, A.J. Tria, The Knee: A Comprehensive Review, World Scientific, 2014.

[10] H. Oonishi, Y. Kadoya, Wear of high-dose gamma-irradiated polyethylene in total hip replacements, J. Orthop. Sci. 5 (3) (2000) 223–228.

[11] H. Oonishi, M. Kuno, E. Tsuji, A. Fujisawa, The optimum dose of gamma radiation–heavy doses to low wear polyethylene in total hip prostheses, J. Mater. Sci. – Mater. Med. 8 (1) (1997) 11–18.

[12] L.S. Bargmann, B.C. Bargmann, J.P. Collier, B.H. Currier, M.B. Mayor, Current sterilization and packaging methods for polyethylene, Clin. Orthop. Relat. Res. 369 (1999) 49–58.

[13] H. McKellop, F.w. Shen, B. Lu, P. Campbell, R. Salovey, Development of an extremely wear-resistant ultra high molecular weight polythylene for total hip replacements, J. Orthop. Res. 17 (2) (1999) 157–167.

[14] O.K. Muratoglu, C.R. Bragdon, D.O. O'Connor, M. Jasty, W.H. Harris, A novel method of cross-linking ultra-high-molecular-weight polyethylene to improve wear, reduce oxidation, and retain mechanical properties: recipient of the 1999 HAP Paul Award, J. Arthroplasty 16 (2) (2001) 149–160.

[15] A. Galvin, E. Ingham, J. Fisher, Wear of Crosslinked UHMWPE in a Hip Joint Simulator, World Tribology Congress III, American Society of Mechanical Engineers, 2005, pp. 617–618.

[16] E.W. Paxton, M.C. Inacio, R.S. Namba, R. Love, S.M. Kurtz, Metal-on-conventional polyethylene total hip arthroplasty bearing surfaces have a higher risk of revision than metal-on-highly crosslinked polyethylene: results from a US registry, Clin. Orthop. Relat. Res.® 473 (3) (2015) 1011–1021.

[17] M.D. Ries, Highly cross-linked polyethylene the debate is over—in opposition, J. Arthroplasty 20 (2005) 59–62.

[18] M. Jasty, H.E. Rubash, O. Muratoglu, Highly cross-linked polyethylene: the debate is over—in the affirmative, J. Arthroplasty 20 (2005) 55–58.

[19] E.W. Paxton, M.C. Inacio, S. Kurtz, R. Love, G. Cafri, R.S. Namba, Is there a difference in total knee arthroplasty risk of revision in highly crosslinked versus conventional polyethylene?, Clin Orthop. Relat. Res.® 473 (3) (2015) 999–1008.

[20] L. Renner, M. Faschingbauer, F. Boettner, Is there a rationale to use highly cross-linked polyethylene in posterior—stabilized total knee arthroplasty?, Ann Transl. Med. 3 (5) (2015).

[21] V.I. Sakellariou, P. Sculco, L. Poultsides, T. Wright, T.P. Sculco, Highly cross-linked polyethylene may not have an advantage in total knee arthroplasty, HSS J.® 9 (3) (2013) 264–269.

[22] J.T. Hodrick, E.P. Severson, D.S. McAlister, B. Dahl, A.A. Hofmann, Highly crosslinked polyethylene is safe for use in total knee arthroplasty, Clin. Orthop. Relat. Res. 466 (11) (2008) 2806–2812.

[23] I.R. Williams, M.B. Mayor, J.P. Collier, The impact of sterilization method on wear in knee arthroplasty, Clin. Orthop. Relat. Res. 356 (1998) 170–180.

[24] L. Costa, P. Bracco, E.B. Del Prever, Physicochemical and mechanical properties of UHMWPE 45 years' experience, Interact. Surg. 2 (3–4) (2007) 169–173.

[25] O.K. Muratoglu, K.K. Wannomae, S.L. Rowell, B.R. Micheli, H. Malchau, Ex vivo stability loss of irradiated and melted ultra-high molecular weight polyethylene, J. Bone Joint Surg. Am. 92 (17) (2010) 2809–2816.

[26] S.L. Rowell, C.R. Reyes, H. Malchau, O.K. Muratoglu, In vivo oxidative stability changes of highly cross-linked polyethylene bearings: an ex vivo investigation, J. Arthroplasty 30 (10) (2015) 1828–1834.

[27] E. Oral, B.W. Ghali, A. Neils, O.K. Muratoglu, A new mechanism of oxidation in ultrahigh molecular weight polyethylene caused by squalene absorption, J. Biomed. Mater. Res. B Appl. Biomater. 100 (3) (2012) 742–751.

[28] S.D. Reinitz, B.H. Currier, D.W. Van Citters, R.A. Levine, J.P. Collier, Oxidation and other property changes of retrieved sequentially annealed UHMWPE acetabular and tibial bearings, J. Biomed. Mater. Res. B Appl. Biomater. 103 (3) (2015) 578–586.

[29] A. Edidin, C. Jewett, A. Kalinowski, K. Kwarteng, S. Kurtz, Degradation of mechanical behavior in UHMWPE after natural and accelerated aging, Biomaterials 21 (14) (2000) 1451–1460.

[30] M.L. Villarraga, A.A. Edidin, M. Herr, S.M. Kurtz, Multiaxial Fatigue Behavior of Oxidized and Unoxidized UHMWPE During Cyclic Small Punch Testing at Body Temperature, Crosslinked and Thermally Treated Ultra-High Molecular Weight Polyethylene for Joint Replacements, ASTM International, 2004.

[31] J.D. Wernlé, J.L. Gilbert, Micromechanics of shelf-aged and retrieved UHMWPE tibial inserts: indentation testing, oxidative profiling, and thickness effects, J. Biomed. Mater. Res. B Appl. Biomater. 75 (1) (2005) 113–121.

[32] D. Baker, R. Hastings, L. Pruitt, Study of fatigue resistance of chemical and radiation crosslinked medical grade ultrahigh molecular weight polyethylene, J. Biomed. Mater. Res. 46 (4) (1999) 573–581.

[33] D. Baker, A. Bellare, L. Pruitt, The effects of degree of crosslinking on the fatigue crack initiation and propagation resistance of orthopedic-grade polyethylene, J. Biomed. Mater. Res., Part A 66 (1) (2003) 146–154.

[34] S.M. Kurtz, H.A. Gawel, J.D. Patel, History and systematic review of wear and osteolysis outcomes for first-generation highly crosslinked polyethylene, Clin. Orthop. Relat. Res.® 469 (8) (2011) 2262–2277.

[35] W. Blömer, E. Lohrmann, Verschleißbeständigkeit von UHMWPE-Artikulationen in der Hüftgelenksendoprothetik, in: S. Weller, A. Braun, C. Eingartner, F. Maurer, K. Weise, E. Winter, R. Volkmann (Eds.), Das BICONTACT Hüftendoprothesensystem, 2007, 1987, pp. 94–100.

[36] E. Gomez-Barrena, J.-A. Puertolas, L. Munuera, Y.T. Konttinen, Update on UHMWPE research from the bench to the bedside, Acta Orthop. 79 (6) (2008) 832–840.

[37] R.W. Hood, T.M. Wright, A.H. Burstein, Retrieval analysis of total knee prostheses: a method and its application to 48 total condylar prostheses, J. Biomed. Mater. Res. 17 (5) (1983) 829–842.

[38] G. Strobl, W. Hagedorn, Raman spectroscopic method for determining the crystallinity of polyethylene, J. Polym. Sci.: Polym. Phys. Ed. 16 (7) (1978) 1181–1193.

[39] F. Rull, A. Prieto, J. Casado, F. Sobron, H. Edwards, Estimation of crystallinity in polyethylene by Raman spectroscopy, J. Raman Spectrosc. 24 (8) (1993) 545–550.

[40] C.C. Naylor, R.J. Meier, B.J. Kip, K.P. Williams, S.M. Mason, N. Conroy, D.L. Gerrard, Raman spectroscopy employed for the determination of the intermediate phase in polyethylene, Macromolecules 28 (8) (1995) 2969–2978.

[41] A. Standard, F2102-06, Standard guide for evaluating the extent of oxidation in ultra-high-molecular-weight polyethylene fabricated forms intended for surgical implants, 2006.

[42] L. Puppulin, Y. Miura, E. Casagrande, M. Hasegawa, Y. Marunaka, S. Tone, A. Sudo, G. Pezzotti, Validation of a protocol based on Raman and infrared

spectroscopies to nondestructively estimate the oxidative degradation of UHMWPE used in total joint arthroplasty, Acta Biomater. (2016).
[43] N.H. Kelly, R.H. Fu, T.M. Wright, D.E. Padgett, Wear damage in mobile-bearing TKA is as severe as that in fixed-bearing TKA, Clin. Orthop. Relat. Res.® 469 (1) (2011) 123–130.
[44] L. Costa, P. Bracco, E.B. Del Prever, M. Luda, L. Trossarelli, Analysis of products diffused into UHMWPE prosthetic components in vivo, Biomaterials 22 (4) (2001) 307–315.
[45] S.C. Scholes, E. Kennard, R. Gangadharan, D. Weir, J. Holland, D. Deehan, T.J. Joyce, Topographical analysis of the femoral components of ex vivo total knee replacements, J. Mater. Sci. – Mater. Med. 24 (2) (2013) 547–554.
[46] O.K. Muratoglu, J. Ruberti, S. Melotti, S.H. Spiegelberg, E.S. Greenbaum, W.H. Harris, Optical analysis of surface changes on early retrievals of highly cross-linked and conventional polyethylene tibial inserts, J. Arthroplasty 18 (2003) 42–47.
[47] A.A. Edidin, M.L. Villarraga, M. Herr, S.M. Kurtz, Multiaxial fatigue behavior of oxidized and unoxidized UHMWPE during cyclic small punch testing at body temperature, J. ASTM Int. 1 (1) (2004) 1–19.
[48] O.K. Muratoglu, C.R. Bragdon, M. Jasty, D.O. O'Connor, R.S. Von Knoch, W.H. Harris, Knee-simulator testing of conventional and cross-linked polyethylene tibial inserts, J. Arthroplasty 19 (7) (2004) 887–897.
[49] P. Barbour, M. Stone, J. Fisher, A study of the wear resistance of three types of clinically applied UHMWPE for total replacement hip prostheses, Biomaterials 20 (22) (1999) 2101–2106.
[50] V. Saikko, Wear of polyethylene acetabular cups against zirconia femoral heads studied with a hip joint simulator, Wear 176 (2) (1994) 207–212.
[51] S.M. Kurtz, L.A. Pruitt, D.J. Crane, A.A. Edidin, Evolution of morphology in UHMWPE following accelerated aging: the effect of heating rates, J. Biomed. Mater. Res. 46 (1) (1999) 112–120.
[52] S. Kurtz, C. Rimnac, L. Pruitt, C. Jewett, V. Goldberg, A. Edidin, The relationship between the clinical performance and large deformation mechanical behavior of retrieved UHMWPE tibial inserts, Biomaterials 21 (3) (2000) 283–291.
[53] S. Bhateja, E. Andrews, S. Yarbrough, Radiation induced crystallinity changes in linear polyethylenes: long term aging effects, Polym. J. 21 (9) (1989) 739–750.
[54] K.K. Wannomae, S. Bhattacharyya, A. Freiberg, D. Estok, W.H. Harris, O. Muratoglu, In vivo oxidation of retrieved cross-linked ultra–high-molecular-weight polyethylene acetabular components with residual free radicals, J. Arthroplasty 21 (7) (2006) 1005–1011.
[55] C. Wolf, C. Macho, K. Lederer, Accelerated ageing experiments with crosslinked and conventional ultra-high molecular weight polyethylene (UHMW-PE) stabilised with α-tocopherol for total joint arthroplasty, J. Mater. Sci. – Mater. Med. 17 (12) (2006) 1333–1340.
[56] M.F. Butler, A.M. Donald, A.J. Ryan, Time resolved simultaneous small-and wide-angle X-ray scattering during polyethylene deformation—II. Cold drawing of linear polyethylene, Polymer 39 (1) (1998) 39–52.
[57] N. Brooks, A. Unwin, R. Duckett, I. Ward, Double yield points in polyethylene: structural changes under tensile deformation, J. Macromol. Sci. Part B Phys. 34 (1–2) (1995) 29–54.
[58] M.F. Butler, A.M. Donald, W. Bras, G.R. Mant, G.E. Derbyshire, A.J. Ryan, A real-time simultaneous small-and wide-angle X-ray scattering study of in-situ deformation of isotropic polyethylene, Macromolecules 28 (19) (1995) 6383–6393.
[59] M.C. Sobieraj, S.M. Kurtz, C.M. Rimnac, Large deformation compression induced crystallinity degradation of conventional and highly crosslinked UHMWPEs, Biomaterials 26 (33) (2005) 6430–6439.
[60] B.H. Currier, J.H. Currier, M.B. Mayor, K.A. Lyford, D.W. Van Citters, J.P. Collier, In vivo oxidation of γ-barrier–sterilized ultra–high-molecular-weight polyethylene bearings, J. Arthroplasty 22 (5) (2007) 721–731.
[61] B.H. Currier, J.H. Currier, M.B. Mayor, K.A. Lyford, J.P. Collier, D.W. Van Citters, Evaluation of oxidation and fatigue damage of retrieved crossfire polyethylene acetabular cups, J. Bone Joint Surg. Am. 89 (9) (2007) 2023–2029.
[62] F.J. Medel, S.M. Kurtz, J. Parvizi, G.R. Klein, M.J. Kraay, C.M. Rimnac, In vivo oxidation contributes to delamination but not pitting in polyethylene components for total knee arthroplasty, J. Arthroplasty 26 (5) (2011) 802–810.
[63] S. Kurtz, Chapter 22: In Vivo oxidation of UHMWPE, in: The UHMWPE handbook: ultra-high molecular weight polyethylene in total joint replacement, second ed., 2009, pp. 325–340.
[64] D.C. Mazzucco, J. Dumbleton, S.M. Kurtz, Can accelerated aqueous aging simulate in vivo oxidation of gamma-sterilized UHMWPE?, J Biomed. Mater. Res. B Appl. Biomater. 79 (1) (2006) 79–85.
[65] S.M. Kurtz, R.L. Siskey, J. Dumbleton, Accelerated aqueous aging simulation of in vivo oxidation for gamma-sterilized UHMWPE, J. Biomed. Mater. Res. B Appl. Biomater. 90 (1) (2009) 368–372.
[66] S.M. Kurtz, W.J. Hozack, J.J. Purtill, M. Marcolongo, M.J. Kraay, V.M. Goldberg, P. F. Sharkey, J. Parvizi, C.M. Rimnac, A.A. Edidin, Otto Aufranc Award Paper: significance of in vivo degradation for polyethylene in total hip arthroplasty, Clin. Orthop. Relat. Res. 453 (2006) 47–57.
[67] D.I. Bower, W. Maddams, The Vibrational Spectroscopy of Polymers, Cambridge University Press, 1992.